MOTORCYCLE CHASSIS ANALYSIS

Diogo Rechena (diogo.rechena@ist.utl.pt)[a]; Luís Sousa (lsousa@dem.ist.utl.pt)[a]; Luís Eça (luis.eca@dem.ist.utl.pt)[a];

[a]IDMEC/IST, Institute of Mechanical Engineering, Instituto Superior Técnico, University of Lisbon, Portugal

Abstract

This paper is intended to provide an overview of a chassis for the future motorcycle PR7 for the AJP brand. With this purpose loads and safety factors will be estimated for later use in several structural analysis. The several components will be analysed separately instead of as a whole and, in some cases, the reaction forces in boundary areas of some parts will be used as external loads in other ones. The structural analysis will be comprised of static simulations for all the components and buckling analysis for parts under compressive loads. The method applied for this structural analysis will be the finite element method in the SolidWorks 2014 software whose CAD functions will also be used in order to provide alternate geometries for the motorcycle.

Keywords: Buckling, CAD, CAE, Chassis, Finite Element Method, Structural Analysis

1 Introduction

1.1 The Company, AJP

Founded in 1987 by António Pinto, AJP came out with its first endure motorcycle, ARIANA 125cc. Since then, the brand has participated in the National Championship great success including five consecutive championships between 1996 and 2000. Since then, the brand has released three more models, all in the 125cc and 250cc categories of dual sport motorcycles [1].

1.2 Dual Sport Motorcycles

Dual Sport motorcycles are a type of PTW vehicle that are fit to drive on and off road needing only different tunings to adapt to different trails although certain characteristics are more fit to drive on asphalt than on dirt such as higher weight, lower and wider seats and more city oriented tyres [2].

1.3 Modelling Motorcycle Chassis

1.3.1 Yielding, Buckling and Fatigue

Metallic alloys have a distinct behaviour characterized by a plastic behaviour preceded by an elastic one. Usually, structures are intended to work under elastic behaviour, which means that the yield stress must not be exceeded. To analyse if the stresses don't exceed the yielding threshold the Von Mises criterion.

$$\frac{S_y}{n} \geq \sqrt{\frac{(\sigma_{xx}-\sigma_{yy})^2+(\sigma_{xx}-\sigma_{zz})^2+(\sigma_{yy}-\sigma_{zz})^2+6(\sigma_{xy}^2+\sigma_{xz}^2+\sigma_{yz}^2)}{2}} \quad (1)$$

Usually in mechanical engineering, structures aren't under static loads, which means fatigue analysis must be performed in order to ensure that cracks are propagating in a controlled rate, which is critical mainly on aluminium alloys. Still, due to the fact that there isn't enough data about the metals, fatigue will only be taken into consideration as a way of evaluating details on the geometry [3].

Also associated with dynamic loads is the buckling phenomenon which occurs in this geometries when the applied loads suffer perturbations leading to high displacement deformations resulting in structural collapse. These phenomena can't be analysed with a static analysis which leads to buckling simulations [4].

1.3.2 Triangulation

Motorcycle chassis are usually frame structures, which means they sustain deformation and their configuration affects deeply the stiffness of the global structure. Triangulated frames come up as a solution to the deformation problem since the geometry tends to convert bending loads into axial loads leading to stiffer and lighter structures [5].

1.3.3 Structural Engine

With high displacement engines a typical solution is to use the engine itself as a structural element supporting both the steering column and the rear suspension.

1.3.4 Backbone Frames

This type of frame is usually light, connecting the steering column to the back of the frame using a beam which allows for a relatively stiff structures. The disadvantage of this type of frame is that it can't usually be fitted with bulky engines.

1.3.5 Twin-spar Frames

This type of frame is usually used in track motorcycles allowing for the accommodation of the air filter which leads to heavier structures but that can also withstand very high loads (in comparison to other frames).

2 Modelling the Problem

2.1 Determining External Loads

Since the frame is for a new motorcycle and its conception is still in an early stage the external loads are still uncertain. Still there are similar motorcycles that can provide an estimate for the normal reactions on the wheels so an XT660X was used to estimate these loads. Also, according to [6] the motorcycle must be able to withstand a total of 186kg of occupants, cargo and accessories. Also, according to [5] the friction coefficient, μ, can reach a maximum value of 1.3 which results in the loads estimated in Table 1.

Fig. 1 – Weighing aa wheel to obtain the reaction value

Table 1 – Loads applied on the motorcycle wheels

Wheel	Reaction (N)	Maximum Friction Force (N)
Front	1500	1750
Back	2500	3250

2.2 Safety Factor

The safety factor was estimated using the Pugsley method, which consists of using several empirical data such as the material quality or the economic impact if failure occurs, yielding two components of the safety factor n_{sx} and n_{sy} of 1.3 and 1.4, respectively, resulting in a project safety factor of 1.82.

Using the material properties of the chosen alloys and the project safety factor the (Table 2) was created.

Table 2 – Material properties

Material	$E\ [GPa]$	ν	$S_y\ [MPa]$	$S_{UTS}\ [MPa]$	$\sigma_{adm}\ [MPa]$
Al	69	0.33	165	250	90
Steel	200	0.29	235	370	129

3 Numerical Analysis and Convergence

In this chapter a convergence analysis will be performed on a loaded component in order to establish the stress and factor of safety precision that will be applied during the analysis of the chassis' several parts.

There are two possible meshing methods present in the SolidWorks software, the standard mesh and the curvature-based one. Both these meshes are going to be tested on the swing arm's connecting rod when subject to a given load.

Table 3 – Changes in stresses with element size variation

Change in mesh size (mm)	1 -1.75	1.75 - 2.5	2.5 - 3.75	3.75 - 5
Curvature-based	0.59%	0.19%	-1.09%	-0.17%
Standard	-0.40%	-1.13%	-1.05%	-3.12%

Table 4 – Changes in FOS with element size variation

Change in mesh size (mm)	1 -1.75	1.75 - 2.5	2.5 - 3.75	3.75 - 5
Curvature-based	35.63%	44.73%	-1.93%	-12.55%
Standard	51.14%	23.24%	23.89%	15.85%

As indicated in Table 3 and Table 4 the curvature-based mesh tends to converge faster than the standard mesh. This is due to the fact that the curvature-based mesh creates elements in circular areas such as holes. Still there are zones where it is not expected to achieve convergence such as corners where the stresses are supposed to tend to infinity, which results in the behaviour shown in (Fig. 2) in which stresses increase in each iteration of mesh refinement.

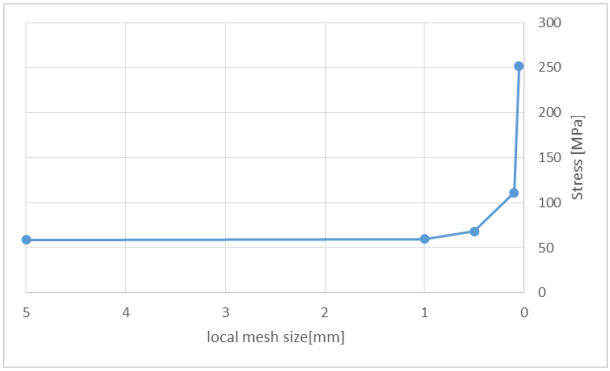

Fig. 2 – Corner stresses in swingarm subject to a 5kN load

4 Initial Geometry Analysis

From the initial geometry, seven subsets were analysed, being these the frontal zone of the frame, which consists of the front suspension (considered a rigid body), the steering column, the oil tank, and the engine's cradle, the swing arm, the engine head's support, the swing arm's rod, the frame's rod, the backbone and, finally the external beams.

4.1 Frontal zone of the Frame

This section proved to be problematic due to the fact that along with stress concentrations in part unions and that the stresses exceeded the allowable stress threshold (Fig. 3) some of the components, such as the oil tank and the oil tank supports were under yielding which is unacceptable in a vehicle structure.

The loads were applied in the front wheel support and the column of the engine's cradle, being the front wheel loads the ones indicated in Table 1 and the column ones 190N in the vertical direction per support, totalling 760N.

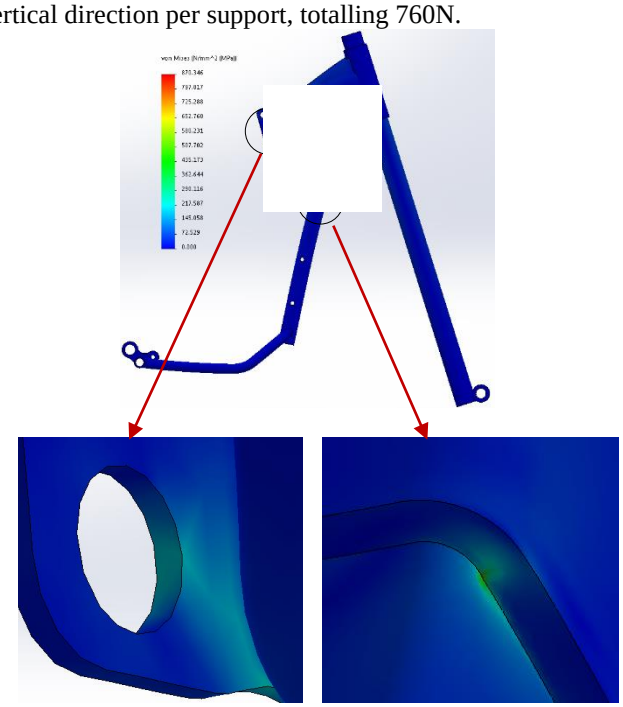

Fig. 3 – Stress concentratcion in the union between the oil tank and the frame's cradle and yielding in the oil tank support

Along with the structural problems, some other issues arose such as the manufacturing of the component. The cradle is made from the union of several beams with welding processes. The current design may cause problems during the welding due to misalignment of components as shown in Fig. 4.

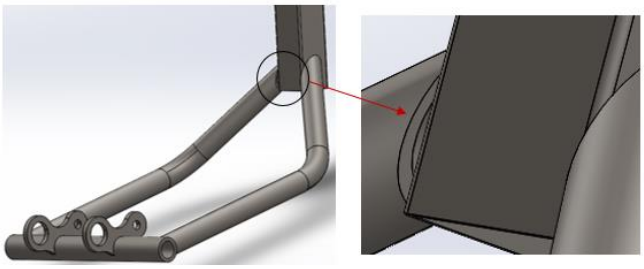

Fig. 4 – Union between the lower beams and the cradle column

After FEA the reactions on the oil tank supports were registered, in order to be used as boundary conditions in the backbone analysis, in Table 5 (Fig. 5).

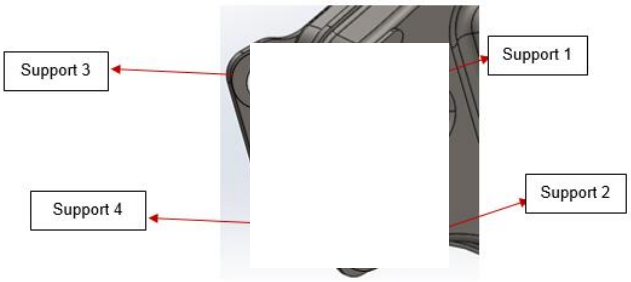

Fig. 5 – Supports in the oil tank

Table 5 – Reaction Forces in the oil tank's supports

	x (N)	y (N)	z (N)
Support 1	202.39	-1721.6	5885
Support 2	-276.3	1693.3	-6651.6
Support 3	206.02	-1711.3	5860.6
Support 4	279.81	1689.2	-6623.6

4.2 Swing Arm

The swing arm (Fig. 6) is a part that connects the rear wheel to the frame and the rear suspension through the swing arm's rod and the frame's rod. To model the loads on this component it was considered that these were applied with the swing arm in the horizontal position in which the bending loads are maximum. After analysis three stress concentration areas were found, two on the swing arm's rod connection and the other one bellow the referred support as shown in Fig. 7.

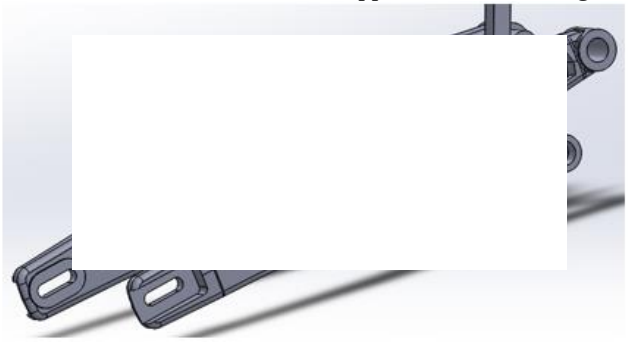

Fig. 6 – Swing arm connected to its rods

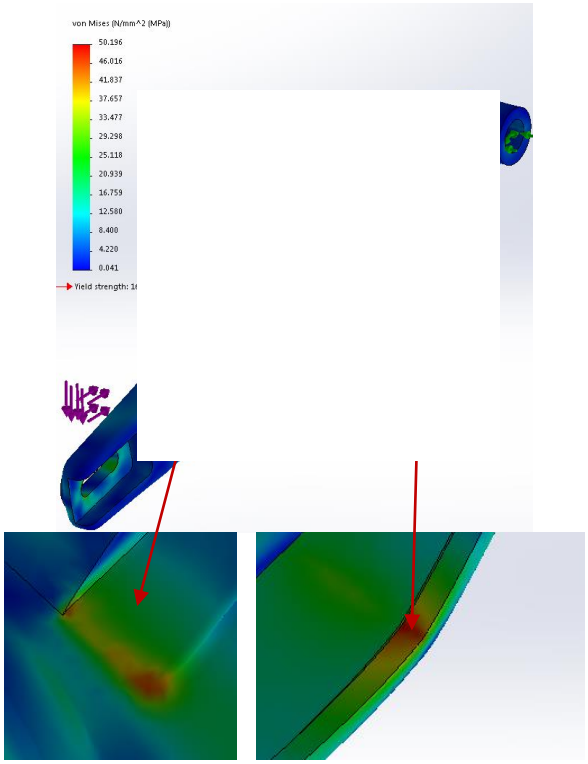

Fig. 7 – Stresses in the swingarm

The most problematic zone is the one in the upper left corner of the support in Fig. 7 since it's manufactured through a milling process in order to generate a corner-like geometry. Still the minimum safety factor is 3.28 (Fig. 8) with a maximum stress of 50MPa. Another factor to take into consideration is buckling, since this component may be subject to compressive loads due to friction forces on the back wheel.

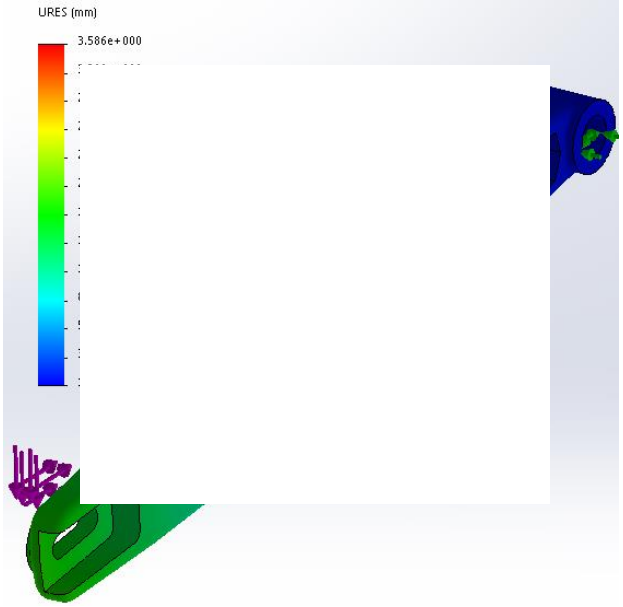

Fig. 8 – Buckling collapse zone for the 4th buckling mode

As shown in Fig. 8 the critical zone is below the swing arm's rod which may prove problematic if mass reducing operations are applied (such as thickness reduction). Still, the minimum positive safety factor for buckling is 52.26 and corresponds to the fourth buckling mode.

4.3 Engine Head's Support

This component (Fig. 9) has the objective of partially supporting the engine's weight. Due to modelling

uncertainties, it was considered that the motorcycle's weight was applied in the engine and that it was equally divided by all of its supports.

After analysis it was confirmed that this component resists yielding since its minimum safety factor is of 5.18 (45 MPa of maximum stress) located in the link to the backbone as shown in Fig. 10.

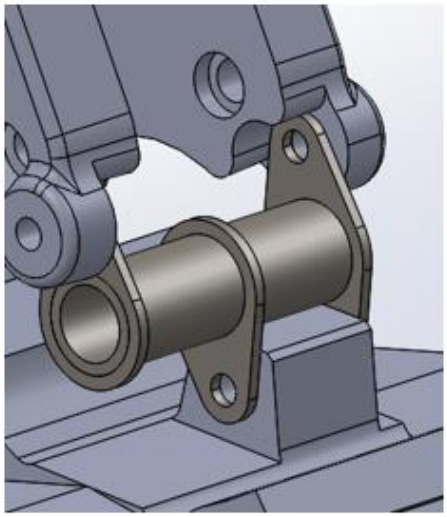

Fig. 9 – Engine Head's Support

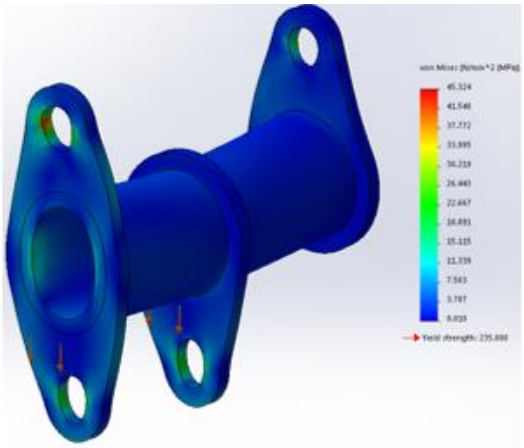

Fig. 10 – Stress concentration in the Engine Head's Support

After analysis the reactions on the links were registered to be used later for the backbone analysis.

Table 6 – Reaction loads on the engine head's support

	x(N)	y(N)	z(N)
Support 1	-12.34	288.78	0.07
Support 2	12.34	91.24	-0.03

4.4 Swing Arm's Rod

This component (Fig. 11) is part of a mechanism formed by the swing arm, the frame's rod and the rear suspension allowing for the reduction of oscillations induced by the pavement on the rear wheel increasing the comfort of the motorcycle and allowing for stability. As the previous two parts, this component is validated with a minimum FOS of 2.71 (Fig. 12) with stresses peaking in the connection with the swing arm with a value of 61MPa.

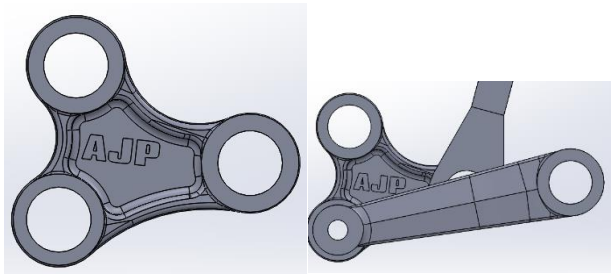

Fig. 11 - Swing arm's rod: part (left) and assembled to frame's rod and rear suspension (right)

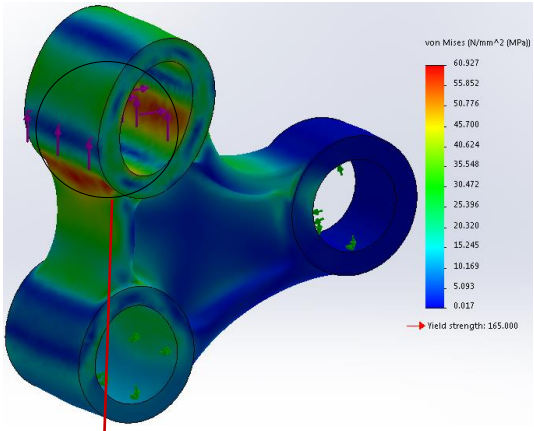

Fig. 12 – Stresses in the swingarm's rod

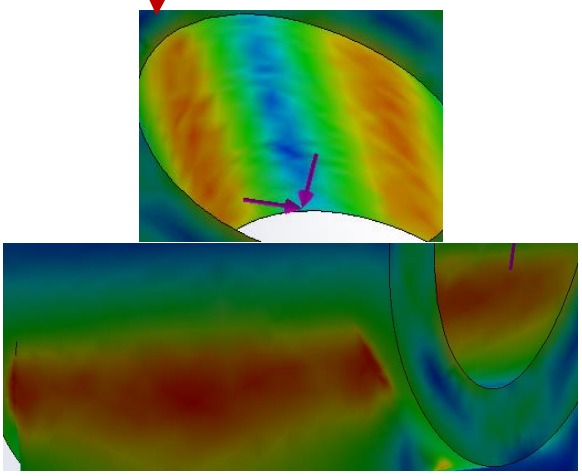

Fig. 13 – Maximum Stresses on the inside and outside of the swing arm's rod

The reaction forces on the link between the swing arm's rod and the frame's rod were taken for later use in the latter's simulation.

Table 7 – Reaction forces on the link between rods

x(N)	y(N)	z(N)
-3580.2	-2437.1	4.9029

4.5 Frame's Rod

The frame's rod connects the swing arm's rod to the engine's cradle working as a pair of bars under compressive/tensile stresses which meant that both loading modes should be analysed and a buckling analysis must be performed for the compressive load. First of all, the loads from the connection to the swing arm's rod must be transformed into its axial equivalent (Fig. 14).

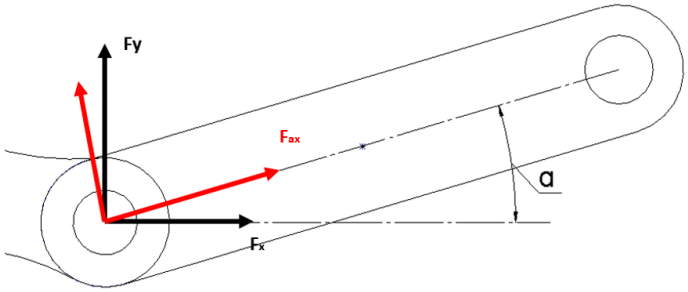

Fig. 14 – Diagram of a rod and the applied loads in different refference frames

From Fig. 14 the axial force may be formulated as:

$$F_{ax} = F_x \cos(\alpha) + F_y \sin(\alpha) \quad (2)$$

With the values from Table 7 and knowing that α≈11.5º it's determined that F_{ax}=1984.9N which is approximated by 2000N. The Static analysis results are presented in Table 8. With Stress concentration areas being, the same for both cases, near the connection to the frame as shown in Fig. 15.

Table 8 – Results for static analysis on the frame's rod

Load Type	Minimum FOS	Maximum FOS
Compressive	9.1	$3.2x10^4$
Tensile	12.4	$1.5x10^4$

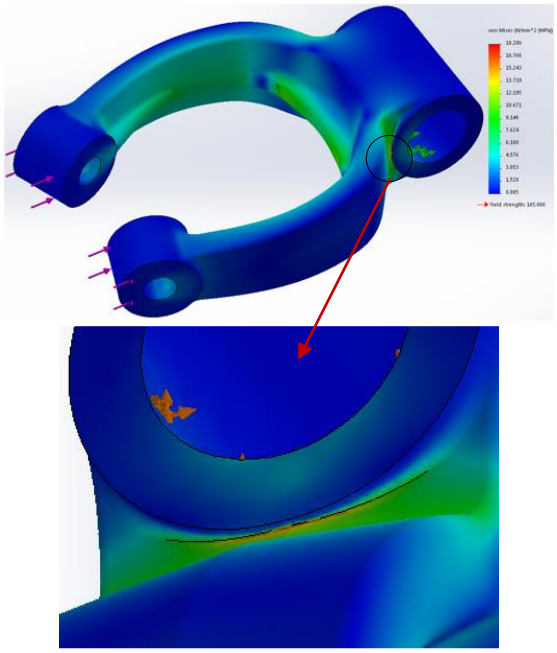

Fig. 15 – Stresses in the frame's rod

As for the buckling analysis, two instability modes stand out for being the ones with minimum positive safety factors that have very close values being them 71.89 and 72.61 for the first and second modes respectively (Fig. 16).

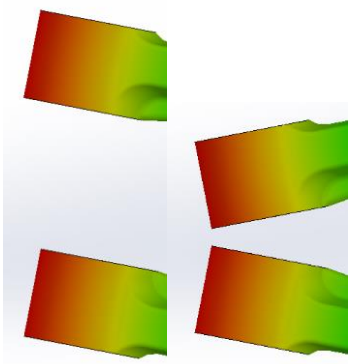

Fig. 16 – First and second buckling modes

4.6 Backbone

The backbone of the frame (Fig. 17) is the component with the most complex set of loads that will be presented in Table 9. And it connects the oil tank to the rear suspension, external beams and the engine head's support.

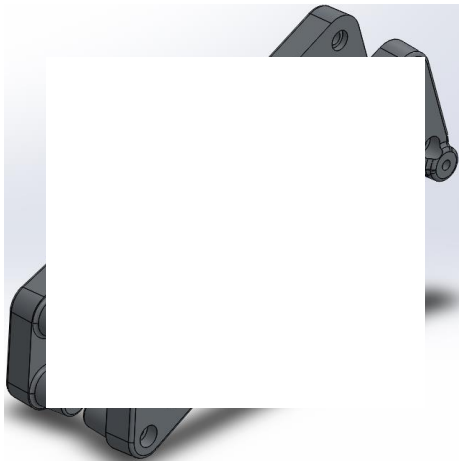

Fig. 17 – Frame's backbone

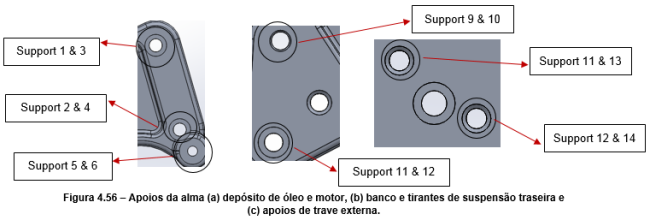

Figura 4.56 – Apoios da alma (a) depósito de óleo e motor, (b) banco e tirantes de suspensão traseira e (c) apoios de trave externa.

Fig. 18 - Backbone support numbering

Table 9 – Loads applied on the frame's backbone

Support	x (N)	y (N)	z (N)
1	-202.39	1721.6	-5885.00
2	276.30	-1693.30	6651.60
3	-206.02	1711.30	-5860.60
4	-279.81	-1689.2	6623.60
5	12.344	-288.78	0
6	-12.339	-91-241	0
7	0	-3150	-3950
8	0	-3150	-3950
9	0	-2250	3950
10	0	-2250	3950

.

This geometry in particular had some issues near the constraint zoned where the stresses tend to infinity even though in reality this doesn't happen. Still it is considered that the component fulfils the static criterion (Fig. 19 and Fig. 20).

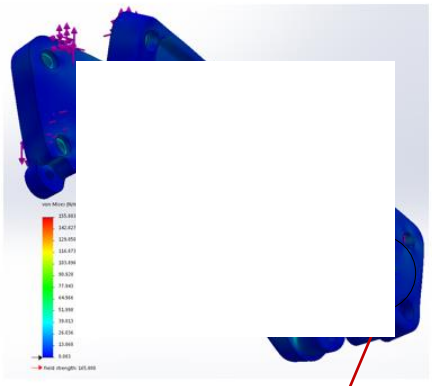

Fig. 19 – Stresses in the backbone

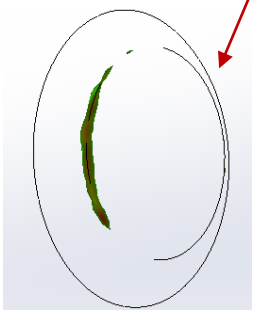

Fig. 20 – Stress concentration in a corner

The reaction loads on the external beams are presented in Table 10.

Table 10 – Reaction loads on the external beam supports

Supports	x (N)	y (N)	z (N)
11 – 13	-31.473	-6239	2258.85
12 – 14	247.725	6450	6772

4.7 External Beams

These components (Fig. 21) increase the global stiffness of the structure by connecting the lower side of the engine's cradle to an engine's supporting shaft and the backbone. As the frontal zone of the frame, the external beams also failed the static criterion with safety factors under 1 (Fig. 22) with a maximum stress of 310 MPa. Another aspect to take into account is the fact that this part is manufactured through casting methods. Also the beam's supposed to be hollow but there is no hole present to allow for a core placement which makes the geometry impossible to manufacture.

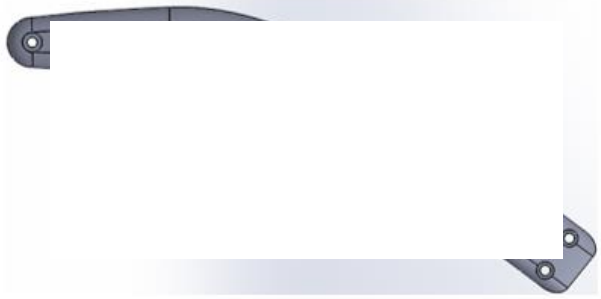

Fig. 21 – External beam geometry

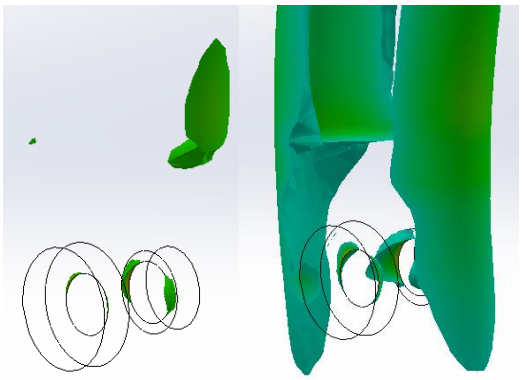

Fig. 22 – Yielding material (left) and material over the allowable stress (right)

5 Geometry improvement

After the initial analysis, some changes were proposed to the initial geometry in some cases with the objective of reducing the component's weight and some others in an attempt to correct the static failure.

5.1 Frontal Zone of the Frame

The only chance made to the frontal zone was discarding the cradle's column and changing the geometry of the oil tank, thus eliminating the connection between these two components (Fig. 23)

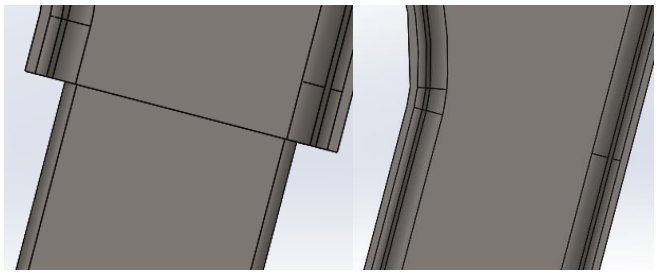

Fig. 23 – Connection between oil tank and cradle's column (left) and modified oil tank (right)

After FEA the stress concentration in the joint zone was eliminated resulting in a more regular stress field (Fig. 24). Still both the oil tank and its supports are still under yielding (264 MPa) resulting in a need to completely change their geometries.

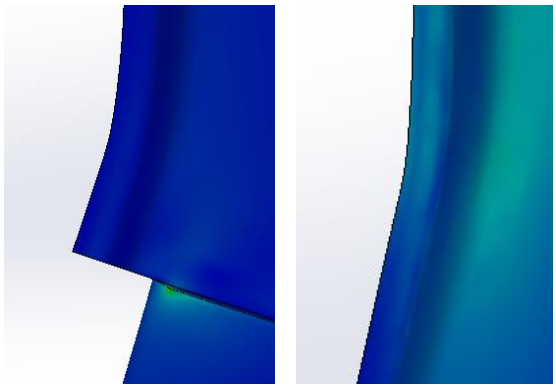

Fig. 24 – Stresses in the join zone before (left) and after (right)

5.2 Swing Arm

The swing arm was completely re-drawn (Fig. 25) adopting a more conventional design with changes on the rear wheel connections as indicated in Fig. 26. The new design has no sharp corners and it also presents a 30.91% reduction in mass. And a maximum safety factor of 1.97.

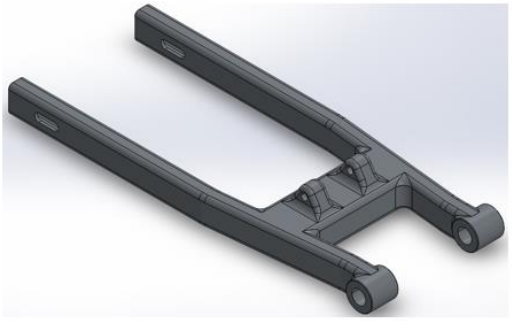

Fig. 25 – New swingarm geometry

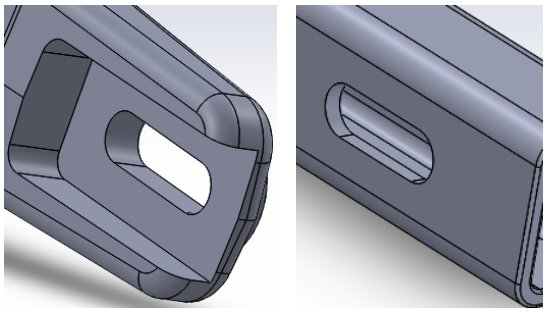

Fig. 26 – Old wheel support (left) and new one (right)

The new component has its maximum stress values near the connection between the arm's beams and near the swing arm's rod support with a maximum value of 84 MPa (Fig. 27)

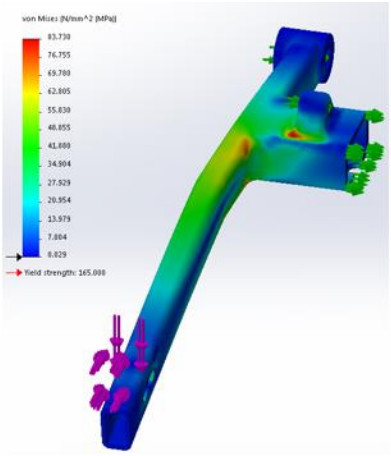

Fig. 27 – Stresses in the new swing arm

After a buckling analysis, the safety factor was reduced to 31.20 with the buckling mode switching from fourth to third.

5.3 Swing Arm's Rod

This rod was also redesigned having only the holes' positions in common with the original part having constant thickness flange and a web thickness reduction from 14mm to 5mm resulting in a component 19.47% lighter than the previous iteration. The minimum safety factor decreased from 2.71 to 1.85 with maximum stresses occurring in the flange connecting the swing arm's support to the frame's rod one (Fig. 28).

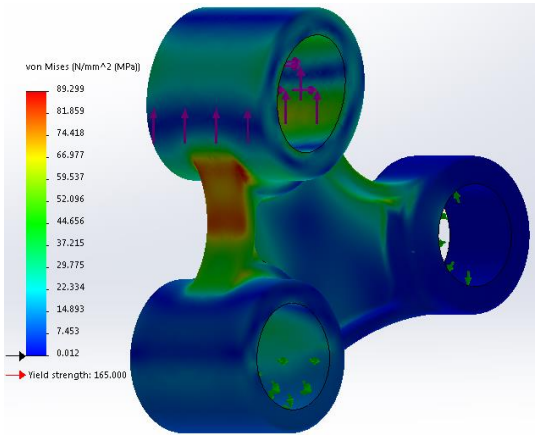

Fig. 28 – Stress concentrations on the rod's flange

5.4 Frame's Rod

As indicated in Table 8 the rod is oversized which leaves room for mass reduction. In order to do so, the original geometry was simplified and re-dimensioned resulting in a 47.40% mass reduction. The new safety factors for static analysis are indicated in Table 11 and the results can be seen in Fig. 29.

Table 11 – Results for the new frame's rod

Load Type	Minimum FOS	Maximum FOS
Compressive	2.29	8.2×10^4
Tensile	2.44	6.9×10^3

There was also a FOS reduction for the buckling criterion with 19.146 and 19.147 for the first and second mode (Fig. 30), respectively. As with the original component, the proximity of these two buckling modes is due to the geometry's symmetry.

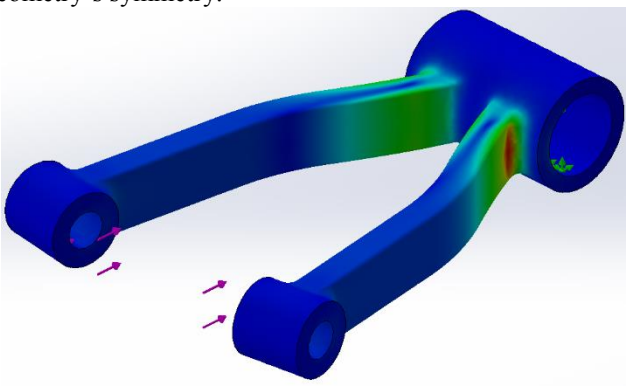

Fig. 29 – Stresses in the new frame's rod

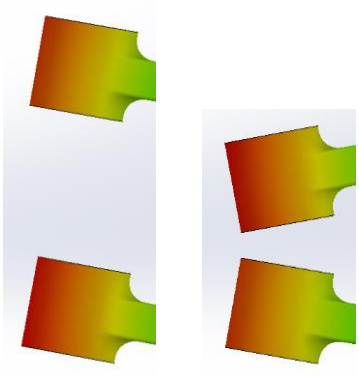

Fig. 30 – First and second buckling modes for the new geometry

5.5 Backbone

Unlike some of the previous components, the backbone wasn't re-designed. Instead the initial geometries were changed maintaining most of its original looks (Fig. 31). One of the major changes to the component was the connection to other parts' configuration, namely the engine head's support as indicated in Fig. 32 which later allowed for thickness reductions in nearby areas of the component. Some of the other supports were also reduced in size in order to eliminate interferences with other details in the geometry such as holes. After the alterations were made the component's mass was reduced in 21.08%

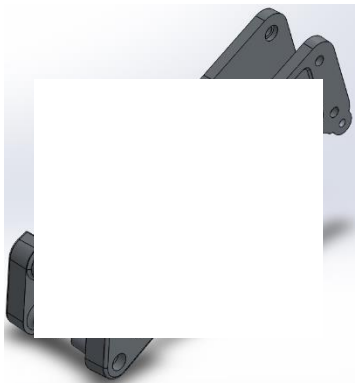

Fig. 31 – New backbone geometry

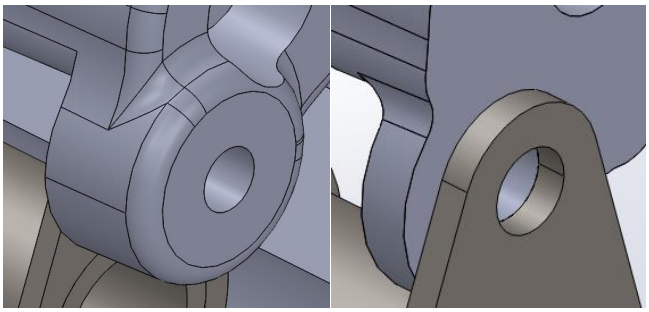

Fig. 32 – Original connection (left) and new one (right)

Fig. 33 – Stresses in the new backbone

After the maximum stress zones shifted to the back of the backbone near the rear suspension supports although stresses also increased in the front, without exceeding the allowable threshold (Fig. 33).

Since the backbone had a significant thickness reduction (up to 56%) it was decided that a buckling analysis was in order which yielded minimum positive safety factors of 33.73 and 33.81 for the seventh and eighth buckling modes (Fig. 34).

Even though the backbone is symmetrical the loads are not but still, the non-symmetrical loads are negligible in comparison with the other ones, which explains the fact that these two modes have similar safety factors.

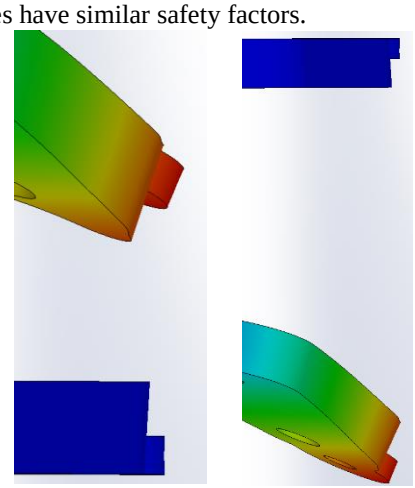

Fig. 34 – Seventh and eighth buckling modes for the backbone

In Table 12 are presented the several mass reductions for the components that were modified with that purpose.

Table 12 – Mass reductions for several frame components

	Mass (g)		Reduction (%)
	initial	final	
Swing Arm	4973.39	3436.14	30.91%
Swing Arm's rod	303.73	244.6	19.47%
Frame's Rod	463.91	244.01	47.40%
Backbone	3880.19	3062.17	21.08%
Total	9621.22	6986.92	27.38%

5.6 External Beams

The only applied change on this part was making it solid instead of hollow (Fig. 35) as an attempt to reduce/eliminate the yielding material.

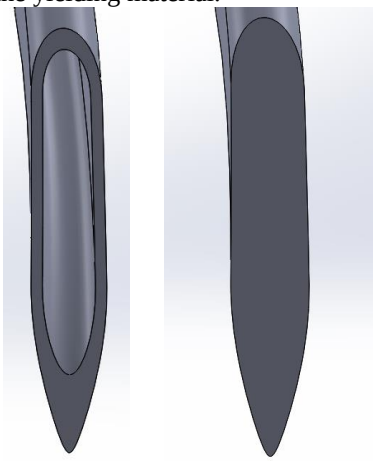

Fig. 35 – Hollow and solid geometries

After finite element analysis a significant reduction in the yielding area was observed but still, there is a significant portion of material with stresses above the allowable limit as shown in Fig. 36 and Fig. 37.

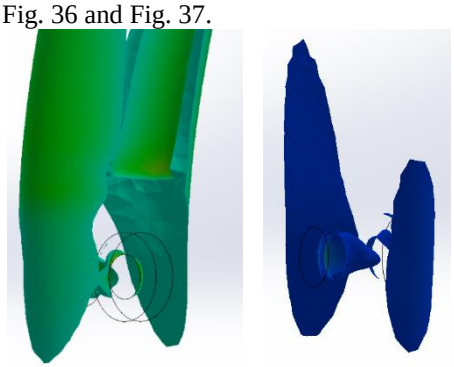

Fig. 36 – Material with stresses above the allowable limit before (left) and after (right)

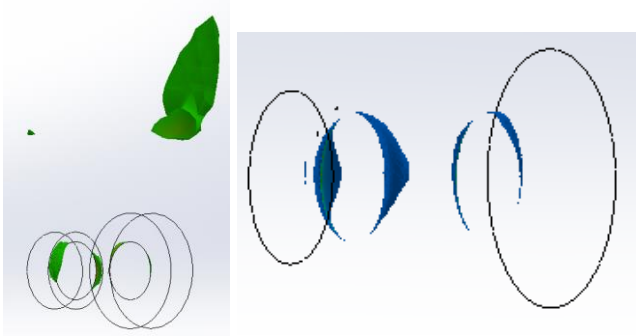

Fig. 37 – Material under yielding in the hollow beam (left) and in the solid one (right)

6 Conclusions

In this paper a structural analysis was provided for a motorcycle frame. To do so an overview of the several types of frames and modelling tools were provided along with the background necessary to perform a finite element analysis.

After these initial considerations the problem was modelled using a similar motorcycle that was used to obtain the maximum loads applied in this new structure. Also, taking into account the bill of materials supplied by the company the allowable stresses were determined for both the steel and aluminium alloys.

A preliminary analysis was then performed on the components in order to identify possibly problematic areas such as yielding zones or geometries that may increase crack initiation and propagation. From this analysis it was concluded that the frontal zone of the frame as well as the external beams didn't meet the yielding criterion although all of the buckling tested parts were validated.

After the preliminary analysis several changes were done to most of the tested components which resulted in a 27% weight reduction in the components that passed the first static and buckling analysis. The frontal zone of the frame and the external beams, even after changes were applied, didn't meet the static threshold meaning that these two components need to be completely redesigned.

Last but not least one detail to take into consideration is the fact that the applied constraints are rigid, which means that the obtained stresses should be higher than the real values since the real components are connected to each other with bolts and weldments.

7 Future Developments

As future work to be done on this chassis, another criterion to take into account is dynamics in order to test if the engine and the road cause resonance on the frame or not [7] e [8]. Also fatigue was not considered in the dimensioning and analysis of the frame. This part of the development of the product is essential since there is no infinite life for aluminium alloys (used in the analysed structure) and the number of mission cycles should be estimated and also the steel components should be designed for infinite life instead of the static criterion only.

Another possibility for model improvement is the measurement of motorcycle loads during standard routes in order to get a better understanding of the vehicle dynamics and how they will affect stresses in the material and the fatigue life of the several components [9].

8 References

1. AJP. *AJP, História*. 2012; Available from: http://www.ajpmotos.pt/.
2. Rider, M.S. *Introduction to Dual Sport Motorcycles*. 2013; Available from: http://motorsportrider.net/Content/mc/NewRider/DualSport.aspx.
3. Branco, C.A.G.M., *MECÂNICA DOS MATERIAIS*. 2ª ed. 1985: Fundação Calouste Gulbenkian. 1098.
4. Simitses, J.G. and D.H. Hodges, *Fundamentals of structural stability*. 1 ed. 2006: Elsevier Science. 480.
5. Foale, T., *Motorcycle Handling and Chassis Design the art and science*. 1 ed. 1984, Spain. 498.
6. Yamaha, *XT660R(W) XT660X(W) Supplementary Service Manual*. 1 ed. 2006.
7. Hugar, N.L. and P.R. Venkatesh, *Shaker based Operating Deflection Shape(ODS) Testing of Two-Wheeler Chassis.* International Journal of Advance Engineer ing and Research Development, 2014. **1**(6): p. 7.
8. Shashanka, S., K.S. Tejaa, S.V. Adithyaa, and K.H. Krishnaa, *Experimental analysis of vibration in a motorcycle footrest.* International Journal of

Mechanical Engineering and Computer Applications, 2013. **1**(3): p. 8.
9. Sener, A.S., *Determination of Vehicle Components Fatigue Life Based on FEA Method and Experimental Analysis.* International Journal of Electronics, Mechanical and Mechatronics Engineering, 2011. **2**(1): p. 13.